Applied Catalysis B: Environmental 209 (2017) 69–79

Contents lists available at ScienceDirect

Applied Catalysis B: Environmental

journal homepage: www.elsevier.com/locate/apcatb

Research paper

Tuning the reduction power of visible-light photocatalysts of gold nanoparticles for selective reduction of nitroaromatics to azoxy-compounds—Tailoring the catalyst support

Qi Xiao*,[1], Zhe Liu, Fan Wang, Sarina Sarina, Huaiyong Zhu*

School of Chemistry, Physics and Mechanical Engineering, Science and Engineering Faculty, Queensland University of Technology, Brisbane, QLD 4001, Australia

ARTICLE INFO

Article history:
Received 25 November 2016
Received in revised form 21 February 2017
Accepted 1 March 2017
Available online 2 March 2017

Keywords:
Selective reduction
Nitroaromatics
Gold nanoparticles
Azoxy-compounds
Photocatalysis

ABSTRACT

It is a challenge to attain high selectivity to azoxy-compounds in the reduction of aromatic nitro compounds as azoxy-compounds can be readily reduced to azo- and aniline compounds. We proposed a new solution to this challenge: gold nanoparticles (AuNPs) on hydrotalcite (HT) support were used to catalyze the reduction under visible light irradiation at ambient temperature; and phosphate (PO_4^{3-}) and metal (such as Ga^{3+}, Fe^{3+}, Zn^{2+}) ions were incorporated into the HT support to moderate the reduction power of the catalyst avoiding the formation of azo- and aniline compounds. Very high azoxy-compound selectivity was achieved under green mild conditions. The photocatalytic activity strongly depends on the incident light wavelength and intensity, and we can further enhance the catalytic efficiency of this photocatalytic process by slight increase in reaction temperature (e.g. 10–20 °C). Moreover, high stability and recyclability of the catalyst were also observed under the investigated conditions. A plausible reaction mechanism was proposed based on the experimental results and literatures. The introduction of both phosphate and metal ions into HT support can prevent the further reduction of azoxy-compounds to azo-compounds or anilines and achieve excellent selectivity to azoxy-compounds. This study reveals that we may engineer a product chemoselectivity by tailoring the supporting materials, and may present a new strategy towards the development of versatile heterogeneous photocatalysts.

1. Introduction

Aromatic azoxy-compounds, which are among one of the most important and central building blocks of naturally occurring compounds and functional materials, have been widely utilized as dyes, analytical reagents, reducing agents, stabilizers, and polymerization inhibitors [1–4]. Moreover, azoxybenzene is the precursor for Wallach rearrangement, which provides a simple way to prepare hydroxyazobenzene and hydroxyazonaphthalene compounds, these compounds are widely used for the coloration of soap, lacquer and resin [5,6]. Generally, azoxy-compounds can be prepared from their corresponding amines, hydroxylamines, azo-, nitro, and nitroso compounds, and the synthesis of these compounds is often conducted at high temperatures or pressures [7–12]. The selective reduction of nitroaromatics to obtain aromatic azo-, azoxy-compounds and anilines has been extensively studied using a variety of heterogeneous catalytic systems recently [11–14]. However, the main products from these processes were intensively focused on anilines or azobenzenes, and the azoxybenzenes were often be regarded as the intermediates during the reduction. Typically, the harsh reaction conditions may result in over-reduced products such as azobenzene or aniline [15,16]. Therefore, for the production of azoxybenzenes, the challenge lies in controlling the selectivity to the target product in the midst of all possible reduction products at a reasonable substrate conversion in order to meet the practical needs, especially under mild conditions. From a green chemistry point of view, it is of great interest to develop highly active, easily separable and reusable catalyst systems that can perform such desirable synthesis of aromatic azoxy-compounds under more controlled, simplified, and greener conditions.

* Corresponding authors.
E-mail addresses: qi.xiao@hdr.qut.edu.au, kevin.xiao@csiro.au (Q. Xiao), hy.zhu@qut.edu.au (H. Zhu).
[1] Present address: CSIRO Manufacturing, Bayview Ave, Clayton, VIC 3168, Australia.

http://dx.doi.org/10.1016/j.apcatb.2017.03.002
0926-3373/

Reduction of nitroaromatics catalyzed by supported AuNPs has been intensively investigated in recent years, thus providing distinct reactivity, activity, and selectivity for the reactions [11–13,17,18]. In 2010, we discovered that the supported AuNPs exhibit superior performance in the photocatalytic reductive coupling of nitro aromatic compounds to produce the corresponding azo- compounds under both visible and UV irradiation [17]. During this process, reductive coupling of nitrobenzene to azoxybenzene firstly took place, and then azobenzene was afforded by loss of the oxygen atom of the azoxybenzene N—O bond. This work highlights that this reductive coupling process can be driven by visible light under ambient conditions. The AuNPs absorb visible light mainly due to the localized surface plasmon resonance (LSPR) effect [19,20]. Very recently, Cu NPs supported on graphene were also been found to exhibit high photocatalytic activity for the reductive coupling of nitroaromatics to aromatic azo-compounds under irradiation of solar spectrum [21]. These work highlighted that the reduction of nitroaromatics can be catalyzed by plasmonic metal NPs such as Au or Cu driven by visible light irradiation under moderate reaction conditions. However, in these processes, the main products are azobenzenes and the selectivity to the intermediate azoxybenzene is not controllable. High-performance catalyst for the selective reduction of nitro compounds to azoxy-compounds (as main product) is still a challenge. We envision that such challenging selectivity requirement prefers catalytic process under mild conditions such as photocatalytic process driven by visible light irradiation. Since the reaction barrier of the final step, reducing azoxybenzene to azobenzene, is higher than that of the other steps in the pathway of the reduction of nitrobenzene to azobenzene [22,23], we have to carefully tune the reduction power of the photocatalysts so that they are able to reduce the first N—O bond but unable to further reduce the azoxy- to azo-compounds. In the present study, we investigated whether the reduction power of AuNP catalyst can be moderated by tailoring the catalyst support to attain high selectivity of azoxy-compound.

HT ($Mg_6Al_2(OH)_{16}CO_3{\cdot}nH_2O$) type layered double hydroxides, which have been demonstrated as a promising support material for AuNP in many catalytic reactions [12,24,25], are known to possess surface basic properties that can be fine-tuned by their compositions [26]. Recently, we successfully prepared Au-Pd alloy NPs on a phosphate (PO_4) modified HT support, and the as-prepared catalysts can efficiently couple the unique basic sites of the support with the photocatalytic properties of the alloy NPs to drive esterification under visible light irradiation [27]. Moreover, it was reported that doping metal cations into HT can afford a strong synergistic effect between AuNPs and HT support, which apparently enhance the catalytic activity [28]. However, the nature of the gold-support interactions and the effects of HT composition on the catalytic performance are still elusive. Lee et al. reported a $BiVO_4$ lattice doped with phosphate to enhance photocatalytic activity, the PO_4 oxoanion dopant greatly improves the charge-transfer characteristics [29]. In view of the likely intermediacy of the azoxy-compound in the selective hydrogenation of nitroaromatics, and considering that the selectivity of the reduction might be tuned in favor of azoxy-products by rational regulation of the synergy between the metal NPs and HT support in the AuNPs catalyzed reaction systems, we were motivated to explore AuNPs deposited on functional HT support with tailored exchanged ions as a catalyst for the selective reduction of aromatic nitro compounds to azoxy-compounds.

In this study, both addition of phosphate anions ($PO_4{}^{3-}$) and metal cations (such as Ga^{3+}, Fe^{3+}, Zn^{2+}) to HT were explored to develop an efficient support for AuNPs, and these modified HT supported AuNP catalysts were found to be efficient visible light photocatalysts for the selective reduction of nitroaromatics to azoxy-compounds under visible light irradiation.

2. Experimental

2.1. Preparation of catalyst

2.1.1. HT support

The Mg-Al HT mixed oxide precursor with an Mg/Al ratio of 3 was provided using a sol-gel process following the procedure described in references with some modification [30,31]. For this, an acidic aqueous solution of metal nitrates was prepared by dissolving $Mg(NO_3)_2{\cdot}6H_2O$ (115.39 g, 0.45 mol) and $Al(NO_3)_3{\cdot}9H_2O$ (56.27 g, 0.15 mol) in 0.6 L of deionized water. A second alkaline solution was prepared from NaOH (60.00 g, 1.5 mol) and Na_2CO_3 (26.50 g, 0.25 mol) in 1.0 L of deionized water. Both solutions were heated to 75 °C. For precipitation, the nitrate and alkaline solutions were added dropwise to 400 mL of water at 75 °C, giving a pH of 10. The suspension was aged for 3 h at 85 °C under vigorous stirring. After cooling to RT, the gel was filtered and loaded into an autoclave. Hydrothermal synthesis was carried out for 16 h at 80 °C. The gel was washed with 350 mL of deionized water until a pH of 7 of the washing water was reached. The white precipitate was freeze-dried and ground.

The HT precursor was calcined to 450 °C (heating rate 10 °C min^{-1}) in a flow of 100 mL min^{-1} synthetic air for 8 h and ready for ion exchange.

2.1.2. PO43–M-HT

A prepared aqueous M^{n+} nitrate solution (0.5 mmol M^{n+}/g HT precursor) was added to the calcined HT precursor in a Schlenk flask. The mixture was stirred at RT for 12 h, then the solid was washed and dried at 110 °C for 10 h, the resultant product was denoted as M-HT. Before doping with $PO_4{}^{3-}$, the M-HT precursors were ground and calcined to 450 °C again in a flow of synthetic air for 8 h. The calcined M-HT (2.0 g) was dispersed into 50 mL Na_3PO_4 aqueous solution (0.02 mmol/L), the mixture was stirred at RT for 12 h, then the solid was washed and dried at 110 °C for 10 h, the resultant solid was ground and denoted as $PO_4{}^{3-}$-M-HT.

2.1.3. Au/PO43–M-HT catalysts

Catalysts with 3 wt% of gold nanoparticles on HT were prepared by impregnation-reduction method. 2.0 g $PO_4{}^{3-}$-M-HT powder was dispersed into 15.2 mL of 0.01 M $HAuCl_4$ aqueous solution while magnetically stirring. 20 mL of 0.53 M lysine was then added into the mixture with vigorous stirring for 30 min. To this suspension, 10 mL of 0.35 M $NaBH_4$ solution was added dropwise in 20 min. The mixture was aged for 24 h and then the solid was separated, washed with water and ethanol, and dried at 60 °C. The dried solid was used directly as catalyst.

2.2. Characterization of catalyst

X-ray diffraction (XRD) patterns of the samples were recorded on a Philips PANalytical X'Pert PRO diffractometer using CuKa radiation (λ=1.5418 Å) at 40 kV and 40 mA. The diffraction data were collected from 5 to 75° with a resolution being 0.01°(2θ). The XPS data were recorded on an ESCALAB 250 spectrometer and AlKa radiation was used as the X-ray source. The C1 s peak at 284.8 eV was used as a reference for the calibration of the binding energy scale. Transmission electron microscopy (TEM) images were taken with a Philips CM200 Transmission electron microscope employing an accelerating voltage of 200 kV. The specimens were fine powders deposited onto a copper microgrid coated with a holey carbon film. The elemental mapping was determined by energy-dispersive X-ray (EDX) spectroscopy attached on an FEI Quanta 200 scanning electron microscope (SEM). The diffuse reflectance

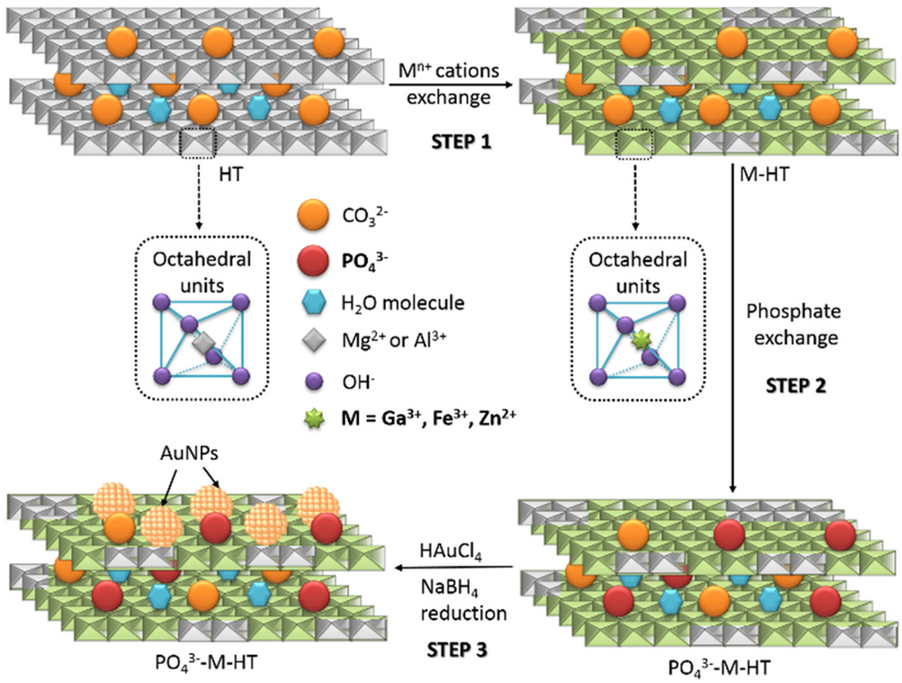

Scheme 1. Preparation of the Au/PO_4^{3-}-M-HT catalysts.

UV/Vis (DR-UV/Vis) spectra were recorded on a Cary 5000 UV/Vis-NIR Spectrophotometer.

2.3. Photocatalytic reaction

The reaction was conducted in a 25 mL round-bottomed Pyrex glass flask with a sealed spigot and a magnetic stirrer. The reaction temperature was controlled by an air-conditioner within a sealed wooden box. A 500 W Halogen lamp was used as the incandescent light source. The light intensity in the reaction position was set at 0.6 W/cm^2 and could be adjusted by changing the distance between the reactor and the light source. The wavelength range was tuned by using various glass filters to cut off the irradiation below a certain value of wavelength. After reaction, 0.5 mL aliquots were collected, and then filtered through a Millipore filter (pore size 0.45 μm) to remove the catalyst particulates. The liquid−phase products were analyzed by an Agilent 6890 gas chromatography (GC) with HP−5 column to measure the change in the concentrations of reactants and products. An Agilent HP5973 mass spectrometer was used to identify the product.

Catalytic reduction of nitrobenzene to azoxybenzene was conducted under the argon atmosphere. Typically, 1.5 mmol nitrobenzene, 15 mL isopropanol as the solvent, and 1.5 mL of 0.1 M KOH solution in isopropanol were mixed in the reactor, followed by adding 50 mg of the catalyst and purging with argon gas, and then stirred during reaction and illuminated with the incandescent light.

3. Results and discussion

The HT precursor was prepared by the homogeneous precipitation method (for details, see Experimental section) [30,31]. A series of phosphate and metal ions modified PO_4^{3-}-M-HT (M = Ga^{3+}, Fe^{3+}, Zn^{2+}) supports was prepared by using the calcination–reconstruction process (utilizing the so-called “memory effect” of HT, see Scheme 1) [27]. Typically, the HT solid was calcined to 450 °C yielding mixed oxides of magnesium and aluminum. When the mixed oxide powder was dispersed into M^{n+} nitrate solution aqueous solution, the layered double hydroxide structure was restored but the M^{n+} cations in solution exchanged with Mg^{2+} or Al^{3+} in the HT solid yielding the M-HT supports with various metal cations (step 1). In order to introduce PO_4^{3-} anions into the support, the as-prepared M-HT precursors were ground and calcined to 450 °C again, and then the mixed oxide powder was dispersed into Na_3PO_4 aqueous solution, the layered double hydroxide structure was restored but the anions between the layers are phosphate anions (step 2). The resultant solid was used as the support of Au NP catalysts. Various HT-supported Au catalysts were prepared by an impregnation-reduction approach with reduction by $NaBH_4$ (step 3). The reduction of a gold salt by $NaBH_4$ has been proven to be an effective method to obtain NPs well-dispersed spheres with mean diameters of ∼10 nm [17,18,27,32–34]. Thus most metal NPs can be conveniently prepared via this method.

The well-defined layered structure characteristic of HT is confirmed for all samples by X-ray diffraction (XRD) patterns (Fig. 1). It is clear that all diffraction peaks could be indexed to the HT structure and the structure remained unchanged after the ion exchanged and Au loaded (Fig. 1). After introducing phosphate and metal ions, the intensity of the diffraction peaks decreased and their widths

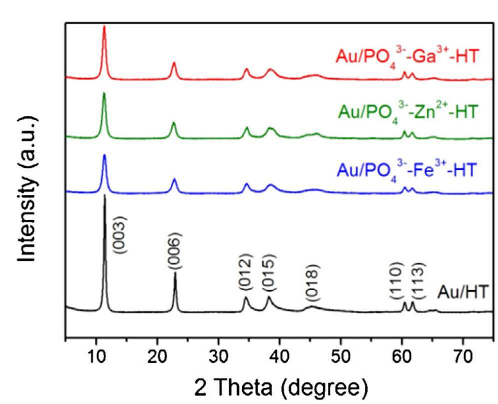

Fig. 1. The XRD patterns of the Au/PO_4^{3-}-M-HT catalysts.

increased (Fig. S1), which indicated a slight decrease of crystallinity of HT support after the ion incorporation. No reflections assignable to Au were present in the XRD patterns, possibly because the low Au content was below the detection limit and/or due to poor crystallinity of the AuNPs on the surface of HT.

Transmission electron microscopy (TEM) images show evidence of high dispersion of AuNPs with mean sizes between 5 and 7 nm (Fig. 2), although a small percentage of larger particles were also observed in some parts of the samples. The overall influence of the support on the AuNP size is relatively small.

The UV/Vis absorption spectra of the as-prepared Au/PO_4^{3-}-M-HT samples are shown in Fig. 3. The HT support exhibits weak absorption of visible light of wavelengths above 400 nm and therefore, the support itself cannot contribute to photocatalytic activity. The absorption peak at 520 nm in the spectrum of the samples is due to the LSPR absorption of the AuNPs [19,20]. The presence of the support and its interaction with the AuNPs can strongly shift and broaden the absorption peaks [25]. Obviously the light absorption of the AuNPs in the visible range is intense due to the LSPR effect, this indicates that the catalysts should possess the ability

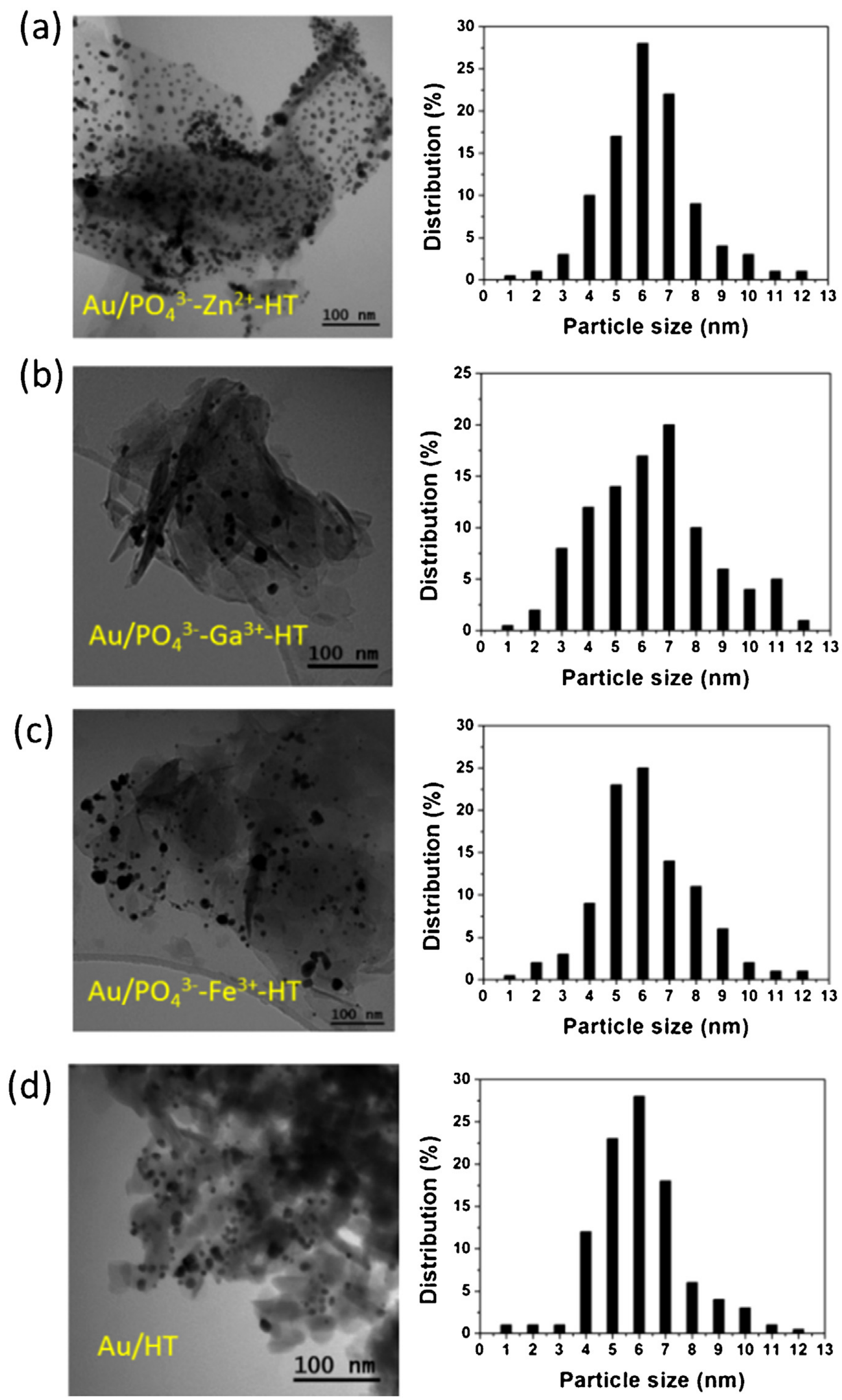

Fig. 2. TEM images and Au particle size distributions for various Au/PO_4^{3-}-M-HT catalysts.

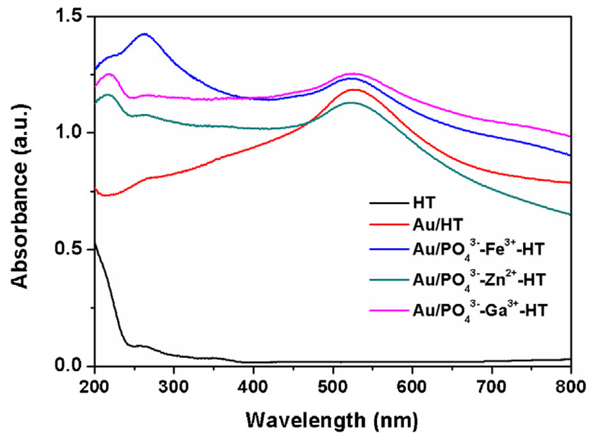

Fig. 3. UV/Vis absorption spectra of as-prepared Au/PO_4^{3-}-M-HT catalysts.

to gain light energy to enhance their catalytic performance when irradiated with visible light.

We applied the obtained Au/PO_4^{3-}-M-HT catalysts for the selective reduction of nitrobenzene reaction under visible light irradiation (Table 1). The reaction was performed in isopropyl alcohol under visible light irradiation with an argon atmosphere at 40 °C for 5 h. Here, isopropyl alcohol is a green solvent, playing the role as the reducing agent in the photocatalytic reduction, which providing hydrogen source and was finally oxidized to acetone [17]. KOH as base is necessary for the reduction of nitrobenzene [17,18,21], the presence of KOH enhances the abstraction of a hydrogen atom from solvent isopropyl alcohol, and facilitates the formation H-Au species [17,35], which is necessary in the catalytic cycle. For comparison control thermal reactions were conducted in the dark and the other experimental conditions kept identical. The parent M-HT, PO_4^{3-}-HT and HT supports did not convert nitrobenzene under identical conditions. Au/HT exhibited excellent selectivity to azoxybenzene (97%) under visible light irradiation (entry 1), this result suggested that the reaction can achieve high azoxy- selectivity using HT support. The Au/PO_4^{3-}-HT catalyst gave very low conversion (4%), but the azoxy- selectivity is extremely high (> 99%, entry 2). Those catalysts with only metal ions in HT also exhibited high azoxy- selectivity, but slightly higher conversions (entries 3–5). Interestingly, when incorporate both the phosphate and metal ion into the HT support, the Au/PO_4^{3-}-M-HT catalysts exhibited much higher activity than the phosphate-free or metal-free catalysts (entries 6–8). More importantly, those reactions catalyzed by Au/PO_4^{3-}-M-HT catalysts exhibited high product selectivity to azoxybenzene (> 97%), compared with that our previously studied Au/ZrO_2 catalyst gave mainly azobenzene selectivity. We use the conversions under visible light irradiation subtracting that in the dark to determine the contribution of light effect (the values in the parentheses in Table 1), all the catalysts with both phosphate and metal ions exhibited obviously increased activity over those without or just with one component of the additive ions (entries 2–8). This confirmed that the phosphate and metal ions play a synergistic effect in the Au/PO_4^{3-}-M-HT catalysts, especially for the reaction under visible light irradiation. For comparison, supported semiconductor catalysts such as Au/ZrO_2 and Au/CeO_2 also give reasonable conversions, but the selectivity to azoxybenzene or the contribution of light effect was poorer (entries 9 and 10). Thus introduction of both phosphate and metal ions into a HT support can result in a promotional effect of the photocatalytic performance for the reduction of nitrobenzene, while maintaining the product selectivity to azoxybenzene.

Considering that Au/PO_4^{3-}-Ga^{3+}-HT photocatalyst exhibited the best performance according to the reaction conversion under light irradiation (entry 8, Table 1), we used it as the model catalyst to further evaluate the reductions by extending the substrate scope. As can be seen from Table 2, Au/PO_4^{3-}-Ga^{3+}-HT can successfully drive several examples of nitroaromatic compounds for reductive coupling yielding corresponding azoxy-compounds with excellent selectivity under visible irradiation. The catalyst exhibited high turnover number (TON) and turnover frequency (TOF) under visible light irradiation for all the reactions catalyzed.

To obtain some insights into the morphology and composition of the Au/PO_4^{3-}-Ga^{3+}-HT catalyst, we further studied the detailed characterization of the catalyst. The high resolution TEM (HR-TEM) image reveals the atom lattices of AuNPs (Fig. 4a). The lattice fringe spacing of 0.236 nm corresponds to the interplanar distance of (111) planes in the Au lattice [36]. The pattern of X-ray photoelectron spectroscopy (XPS) was used to investigate the oxidation states of Au. The Au 4f XPS spectrum (Fig. 4b) reveals the binding energy (BE) of Au $4f_{7/2}$ and Au $4f_{5/2}$ at 83.3 eV and 86.9 eV, respectively. The BE of Au are identical to the bulk of gold metal [37], and the broad peak close to Au$4f_{5/2}$ is due to Al2p

Table 1
The catalytic performance of various AuNP catalysts.

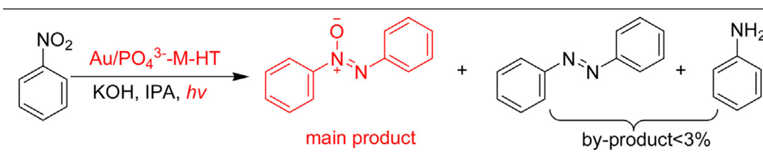

Entry	Catalysts	Light reaction		Dark reaction	
		Conv. (%)	Selec. (%)	Conv. (%)	Selec. (%)
1	Au/HT	42 (13)	97	29	98
2	Au/PO_4^{3-}-HT	4 (2)	>99	2	99
3	Au/Zn^{2+}-HT	16 (13)	>99	3	>99
4	Au/Fe^{3+}-HT	13 (13)	94	0	0
5	Au/Ga^{3+}-HT	13 (5)	>99	8	>99
6	**Au/PO_4^{3-}-Zn^{2+}-HT**	**54 (41)**	**98**	**13**	**86**
7	**Au/PO_4^{3-}-Fe^{3+}-HT**	**52 (40)**	**97**	**12**	**77**
8	**Au/PO_4^{3-}-Ga^{3+}-HT**	**56 (54)**	**>99**	**2**	**>99**
9	Au/ZrO_2	42 (24)	54	18	84
10	Au/CeO_2	30 (4)	94	26	98

Reduction reaction was conducted in an argon atmosphere at 40 °C using 15 mL of isopropyl alcohol(IPA) mixed with 1.5 mL 0.1 M KOH/IPA, 1.5 mmol nitrobenzene, and 50 mg catalyst. Reaction time: 5 h. The light intensity in the reaction position was set at 0.6 W/cm^2. The conversions and selectivity were calculated from the product formed and the reactant converted measured by gas chromatography (GC). The values in the parentheses are the conversion under visible light irradiation subtracting that without light.

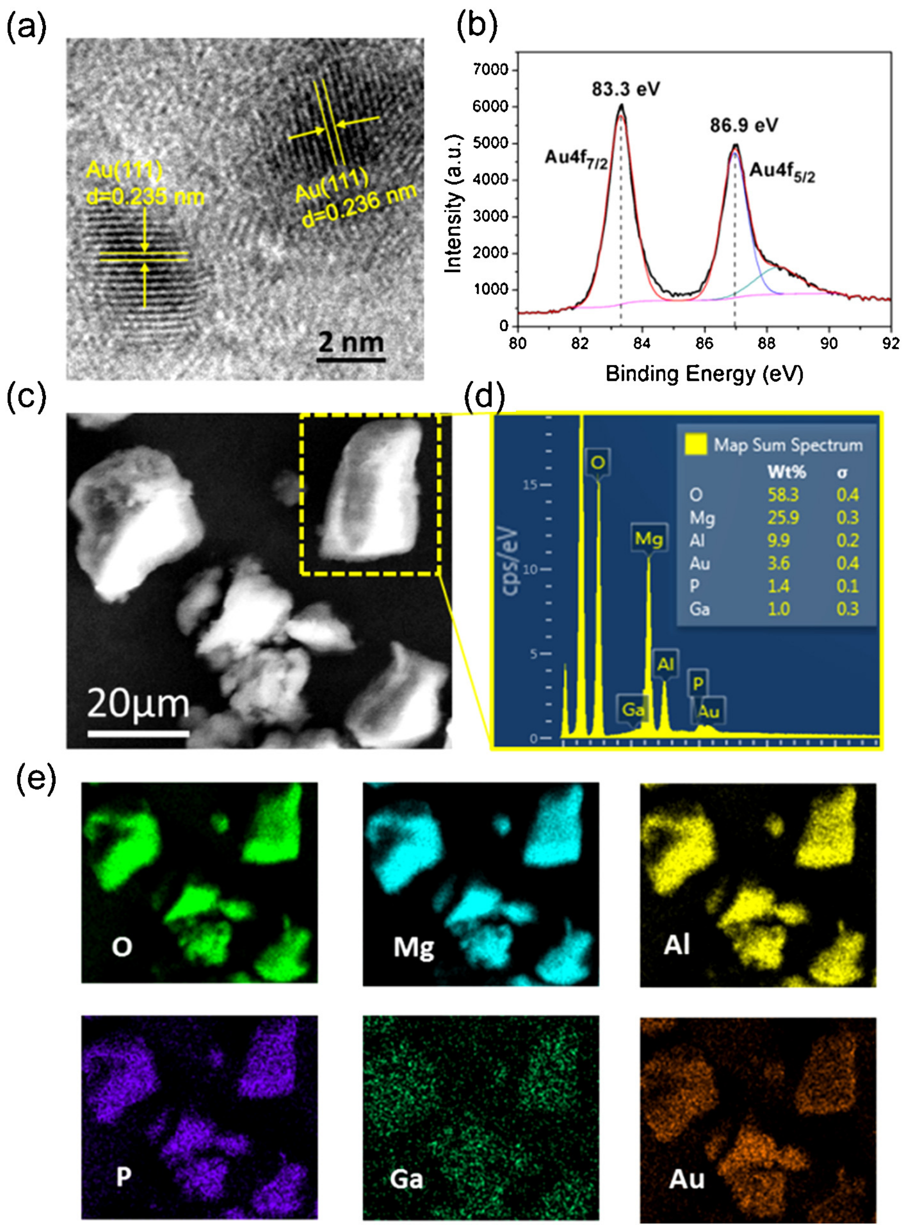

Fig. 4. (a) HR-TEM image of the AuNPs in a typical Au/PO_4^{3-}-Ga^{3+}-HT catalyst. (b) XPS spectra of Au in the Au/PO_4^{3-}-Ga^{3+}-HT catalyst. (c) SEM image of a typical Au/PO_4^{3-}-Ga^{3+}-HT sample. (d) The EDX spectrum as indicated in Fig. 4c. (e) The EDX mapping of O, Mg, Al, P, Ga and Au elements.

energy loss peak. To investigate the elemental composition in the as-prepared photocatalyst, energy-dispersive X-ray spectroscopy (EDX) elemental mappings of the Au/PO_4^{3-}-Ga^{3+}-HT catalyst were performed (Fig. 4c–e). EDX elemental mapping of the Scanning electron microscopy (SEM) image shows that all the components are homogeneously distributed throughout the sample. The phosphorus and gallium elements are clearly evidenced in the mapping data, and the signals indicate that the doped phosphate anions and gallium cations are uniformly distributed in the HT sample. The percentages of Mg, Al, P, Au and Ga elements in the catalysts were also analyzed from the EDX spectrum (Fig. 4d), the Mg/Al ratio (3/1) and Au content (3%) are well matched with the initial experimental design.

A key attraction to heterogeneous catalysis is the possibility of catalyst recycling. We carried out a series of the reduction of nitrobenzene reaction under irradiation to demonstrate the recyclability of Au/PO_4^{3-}-Ga^{3+}-HT catalyst. Briefly, after each reaction cycle, Au/PO_4^{3-}-Ga^{3+}-HT catalyst was separated by centrifugation, and washed thoroughly by ethanol twice and dried for subsequent reactions. As shown in Fig. 5a, the catalyst was reused for 5 cycles without significant loss of activity, and the selectivity to azoxybenzene can be still maintained at a high level. XRD results confirm retention of the original HT structure (Fig. 5b). From the typical TEM image of the Au/PO_4^{3-}-Ga^{3+}-HT catalyst after recycled (inset in Fig. 5b), the AuNPs still distribute evenly on the HT surface, no obvious agglomeration was observed, and the average size and distribution of the AuNPs was unchanged. These results demonstrate that Au/PO_4^{3-}-Ga^{3+}-HT catalyst is stable and practical visible light photocatalyst for reduction of nitrobenzene to azoxybenzene.

In order to better understand the effect of light irradiation, we applied optical filter glass with different cut off wavelength to clarify the influence of wavelength range on the photocatalytic activity of Au/PO_4^{3-}-Ga^{3+}-HT for the reduction reaction. As shown in Fig. 6a, when the light with wavelength below 490 nm was removed (the working wavelength range will be 490–800 nm), the conversion of the reaction decreased to 35%; when cut off the wavelength

Table 2
The Photocatalytic reduction of nitrobenzenes with different substrates using Au/PO_4^{3-}-Ga^{3+}-HT catalyst.

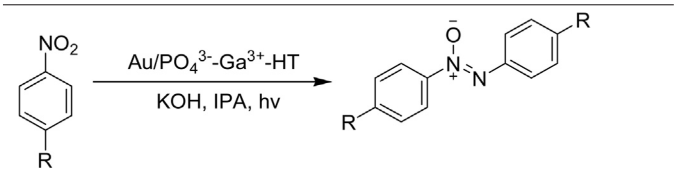

Entry	R	Reaction rate ($mmol\,g_{cat}^{-1}\,h^{-1}$)	Selectivity (%)	TON	TOF (h^{-1})
1	CH_3-	3.36	98	111	22
2	Cl-	3.48	>99	114	23
3	CH_3O-	3.66	96	120	24
4	CH_3CO-	3.60	97	118	24

Reduction reaction was conducted in an argon atmosphere at 40 °C using 15 mL of IPA mixed with 1.5 mL 0.1 M KOH/IPA, 1.5 mmol reactant, and 50 mg catalyst. Reaction time: 5 h. The light intensity in the reaction was set at 0.6 W/cm^2. The reaction rate and selectivity were calculated from the product formed and the reactant converted measured by GC. The reaction rate was calculated based on the converted molecules per gram of catalysts per hour. TON = amount of reactant (mol) × conversion/amount of Au (mol), TOF = TON/reaction time (h).

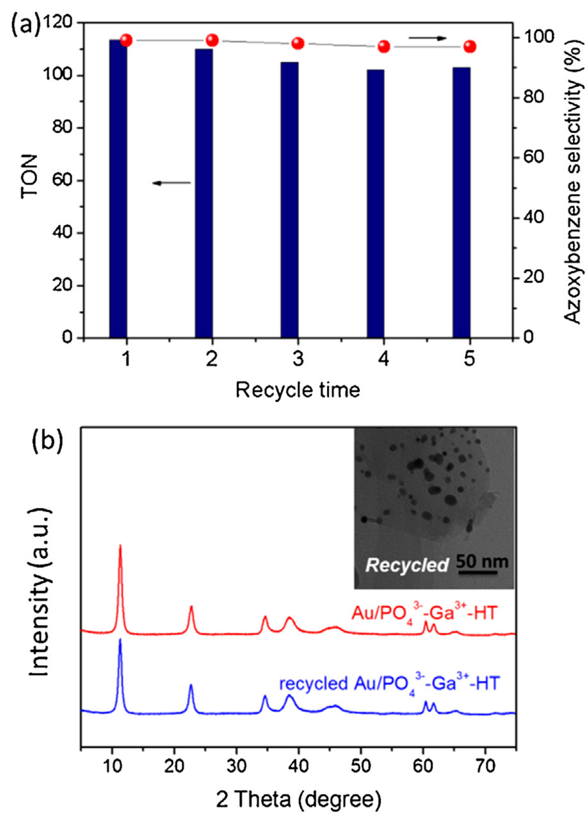

Fig. 5. (a) The photocatalytic activity the Au/PO_4^{3-}-Ga^{3+}-HT catalyst after 5 recycled. (b) XRD patterns comparison of the recycled Au/PO_4^{3-}-Ga^{3+}-HT catalyst. Inset: representative TEM image of the Au/PO_4^{3-}-Ga^{3+}-HT catalyst after recycled.

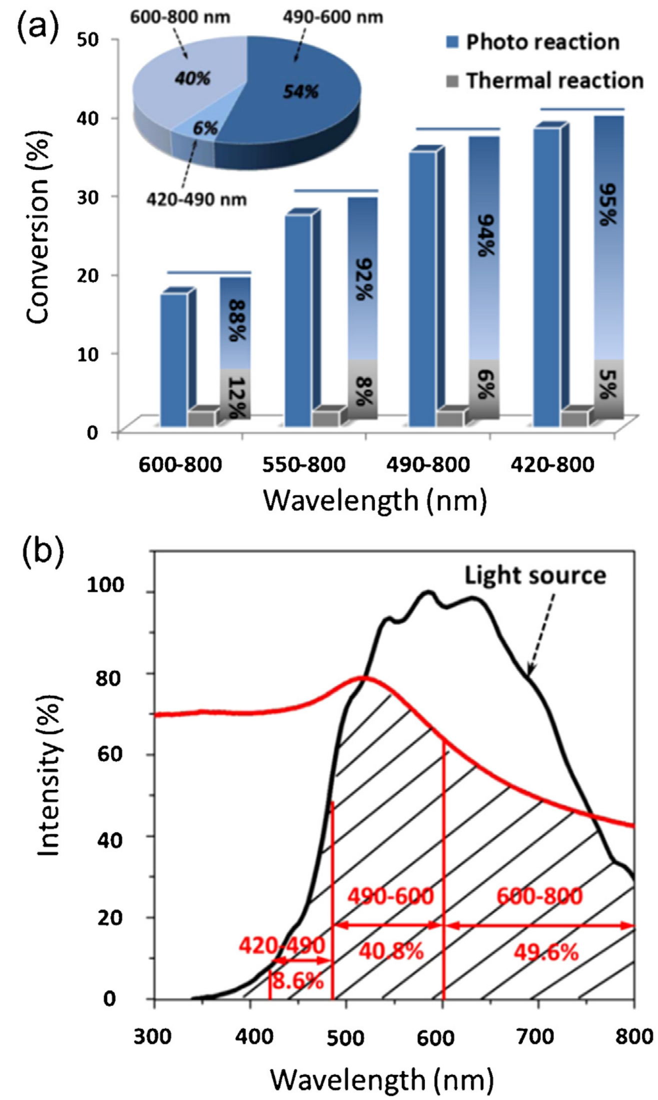

Fig. 6. (a) The dependence of the catalytic activity of the Au/PO_4^{3-}-Ga^{3+}-HT catalyst for the reaction on the wavelength of the light irradiation. Both light driven reaction and the thermal reaction in the dark were conducted at 40 °C. The inset pie chart is the contribution to the conversion efficiency for the specific wavelength ranges used. This was calculated by using the equation: $(C_{short}-C_{long})/(C_{short}-C_{dark})$, where C_{short} is the conversion in the short wavelength range, C_{long} is the conversion in the long wavelength range, and C_{dark} is the conversion in the dark; for example, the contribution in the range of 490–600 nm = $(C_{490}-C_{600})/(C_{490}-C_{dark})$ = (35%–17%)/(35%–2%) = 54%. (b) The energy absorbed by the AuNPs from irradiation was estimated from the overlap area of the absorption spectrum of the AuNP (red curve) with the spectral irradiance of incandescent light used (black curve). (For interpretation of the references to colour in this figure legend, the reader is referred to the web version of this article.)

below 550 nm and 600 nm, the conversion decreased to 27% and 17% respectively; considering that the thermal conversion at this temperature is 2%, we found that the main contribution of light irradiation to the photocatalytic activity comes from light in the range of 490–600 nm, accounts for the 54% of the total conversion rate, while light in the wavelength ranges of 400–490 nm and 600–800 nm contribute 7% and 40%, respectively (pie chart in Fig. 6a). The light energy absorbed by the AuNPs from light in the wavelength range between 490 and 600 nm was estimated from the overlap area of the absorption spectrum of the AuNPs with the spectral irradiance of incandescent light used (Fig. 6b), to be 40.8% of the total light energy absorbed by the NPs. Given that the LSPR peak of AuNPs is in this wavelength range, these results suggest that AuNPs functions as an antenna for visible light absorption.

The impact of the light intensity on the catalytic performance was also investigated while keeping other experimental conditions unchanged. An important feature of the photocatalytic process on metal NP catalysis is that the catalytic activity of the NPs can be increased by slightly elevating the reaction temperature, this is owing to metal NPs have continuous electronic energy levels thus can absorb thermal energy [27,38,39]. Fig. 7a shows the rate of nitrobenzene reduction over the Au/PO_4^{3-}-Ga^{3+}-HT catalyst as a function of light intensity at different temperatures (30, 40, 50 and 60 °C, respectively). When the light intensity increased (the

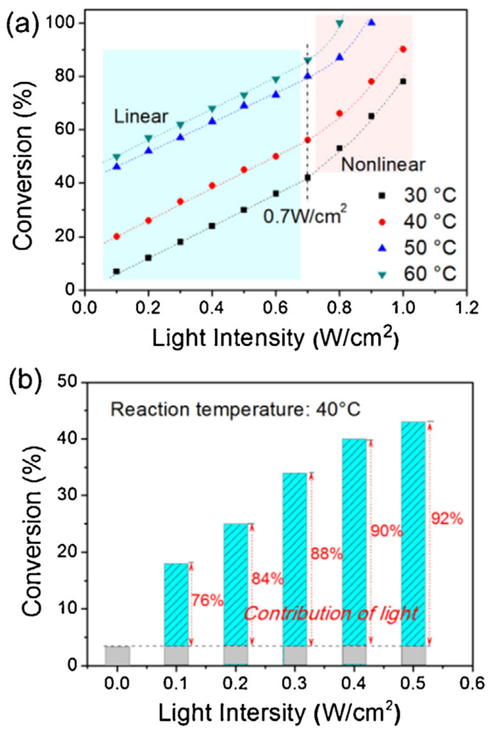

Fig. 7. (a) Photocatalytic rate as a function of light intensity for various temperatures. (b) Light intensity dependent activity of Au/PO_4^{3-}-Ga^{3+}-HT catalyst for the reaction at 40 °C, the percentage numbers in red show the contribution of light irradiation. (For interpretation of the references to colour in this figure legend, the reader is referred to the web version of this article.)

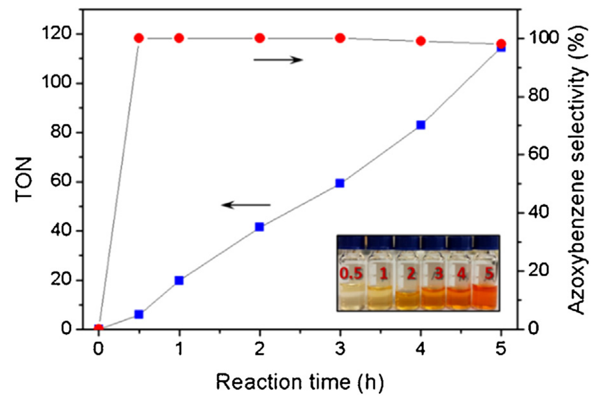

Fig. 8. Time-conversion plot for the nitrobenzene reduction using Au/PO_4^{3-}-Ga^{3+}-HT catalyst under light irradiation; inset: a photograph of the products obtained at different time intervals.

reaction temperature of the reaction mixture was controlled at 45 °C, the only parameter changed was the light intensity), the reaction conversion increased linearly up to a light intensity of 0.7 W/cm^2. Further increase in light intensity results in much greater rate increases, and the relation between light intensity and reaction conversion becomes nonlinear. This is a feature of the chemical processes driven by the light excited electrons of metals [38]. When the reaction was conducted under lower temperature and lower incident light intensity, the light excited electron transfer dominates the photocatalytic activity, which exhibited a nearly linear increase in the photocatalytic activity. At a higher temperature, light excites more conduction electrons of AuNPs to higher energy levels, and the probability of the transfer of the excited electron from the metal to the adsorbed molecules to initiate their reaction is higher than that at lower reaction temperature [39]. In this case, the thermal energy is sufficient to induce a significant population of vibrationally excited states of the reactant molecules to induce the catalytic reaction. Thus at higher temperatures, the contribution from the thermal effect can be greater than that from the irradiation (light excited electrons) as the reactant molecules may gain most energy from heating to overcome the activation energy barrier. Overall, the ensemble effect from both light excited electrons and thermal effect may result in a nonlinear increase in the catalytic performance at higher temperatures and intensities. It is also possible that when the light intensity is very high, multiphoton absorption occurs, increasing the number of excited metal electrons with sufficient energy to drive the reactions [38,39]. To achieve 100% reaction rate, we can simply increase the reaction temperature from 40 to 50 °C under higher intensity of 0.9 W/cm^2 irradiation, the product selectivity remained to azoxybenzene. The results suggest that we can obtain high catalytic efficiency with Au/PO_4^{3-}-Ga^{3+}-HT catalyst driven by light under slightly higher temperature, which represents an apparent merit compared with traditional heterogeneous catalysts and semiconductor photocatalysts.

When the reaction temperature was fixed at 40 °C, the dependence of catalytic activity on light intensity was investigated (Fig. 7b). The light induced enhancement on the conversion was calculated by subtracting the observed conversion of a reaction performed in the dark from the conversion observed under light irradiation controlled at the same temperature (40 °C). This allows the photo-induced and thermal contributions to the conversions to be determined and expressed as a percentage for each process. It shows clearly that higher light intensities, results in a larger light enhanced contribution to the total conversion rate. A greater irradiance provides more light excited energetic electrons and creates a stronger electromagnetic field around the NPs (electromagnetic field enhancement effect), as reported for AuNPs [19,20,40]. At low reaction temperatures, the light-excited electrons play a dominate role, exhibiting linear increase in the catalytic activity. Thus, for many catalyzed reactions in which the interaction of the light-excited hot electrons of a catalyst with reactant molecules induces the reaction, high reaction temperatures are not a prerequisite for efficacy; we may achieve a good catalytic performance by simply increase the incident light intensity at a lower reaction temperature.

To study the reaction mechanism, firstly we studied the evolution of the products during the time course of the catalytic reduction using Au/PO_4^{3-}-Ga^{3+}-HT catalyst under visible light irradiation (Fig. 8). We can see that the reaction conversion increase gradually along with the time prolonged during the reaction, and the selectivity to azoxybenzene approached nearly 100% from the initial reaction stage (0.5 h) and remained constantly until the reaction completed. Oxygen gas was released as an unforeseen by-product, a deflated gas expansion bag was connected to the sealed round-bottom flask in order to collect the gas released throughout the photocatalytic reduction. The collected gas in the bag was then analyzed by GC, we can confirm there is some oxygen released in the reduction process. We can also see clearly the color change during the reaction course from the photograph of the product obtained at different time intervals (inset in Fig. 8). However, these results could not provide a direct explanation for the product selectivity in the reaction.

The generally accepted reaction pathway for the catalytic reduction of aromatic nitro compounds is based on the electrochemical model presented by Haber more than 100 years ago [41]: the nitrobenzene is reduced to the nitrosobenzene and further to the corresponding phenylhydroxylamine in two very fast consecutive steps, and then the coupling of one nitroso compound molecule with an intermediate hydroxylamine molecule to give a

Table 3
Reaction pathway study of catalytic performance using Au/PO_4^{3-}-Ga^{3+}-HT catalyst for various intermediates as substrates.

Entry	Reactant	Reaction time (h)	Conversion (%)	Selectivity (%)	
				Azoxy-	Azo-
1	Nitrosobenzene	2	85	>99	–
2	Phenylhydroxylamine	2	98	54	46
3	Nitrosobenzene+ Phenylhydroxylamine	1	100	98	2
4	Azoxybenzene	6	5	–	100
5	Azobenzene	6	0	–	–

Reduction reaction was conducted in an argon atmosphere at 40 °C using 15 mL of IPA mixed with 1.5 mL 0.1 M KOH/IPA, 1.5 mmol reactant, and 50 mg catalyst. The light intensity in the reaction was set at 0.6 W/cm^2. The reaction rate and selectivity were calculated from the product formed and the reactant converted measured by GC.

azoxybenzene molecule, which is further reduced in the consecutive steps to the corresponding azobenzene, and finally an aniline compound molecule [22,42]. However, the sequence of reactions is rather complex, and the intermediates formed in this process are very reactive species that can react with each other as well as with other chemicals [42]. Although some mechanistic studies were reported on AuNP catalyzed reactions under thermal conditions [12,22], none of these can be used to verify the reaction network observed in the present study, even the photocatalytic pathway for the reduction of nitrobenzene with Au catalyst has not been fully understood yet in our previous study [17]. To gain insight into the reaction pathway of the process with the photocatalyst, reductions of the possible intermediates (nitrosobenzene, phenylhydroxylamine and their mixture) were conducted using Au/PO_4^{3-}-Ga^{3+}-HT catalyst, with the other experimental conditions maintained identical to those for the nitrobenzene reduction (Table 3).

As shown in entry 1, if using nitrosobenzene as the reactant, azoxybenzene was the main product with >99% selectivity. However, when using phenylhydroxylamine as the reactant, the reaction gave higher conversion (98%) within 2 h; but the selectivity to azoxybenzene was only 54%, and the rest product was azobenzene (entry 2). Further experiments using the mixture of nitrosobenzene and phenylhydroxylamine gave high conversion and high azoxybenzene selectivity, and importantly, the reaction proceeded rapidly and completed within 1 h (entry 3). Since both of nitrosobenzene and phenylhydroxylamine are very unstable under the reaction conditions, thus once phenylhydroxylamine was formed in the reaction, it could react with nitrosobenzene to form azoxybenzene. To further confirm whether the reaction will continue to proceed to form azobenzene, we applied azoxybenzene as the reactant for the reaction (entry 4). The reaction was almost sluggish with only 5% conversion for 6 h. When using azobenzene as the reactant, the reaction did not give any conversion (entry 5). These experimental results confirmed that the formation of azoxybenzene is much more favorable when using Au/PO_4^{3-}-Ga^{3+}-HT catalyst under light irradiation.

The proposed mechanism for the visible light driven reduction of nitrobenzene to azoxybenzene is shown in Scheme 2. The hydrogen atom abstracted from isopropyl alcohol is first adsorbed on the AuNP surface, forming relatively stable H–AuNP species [17,43]. The linear dependence of the photo-induced reaction rate

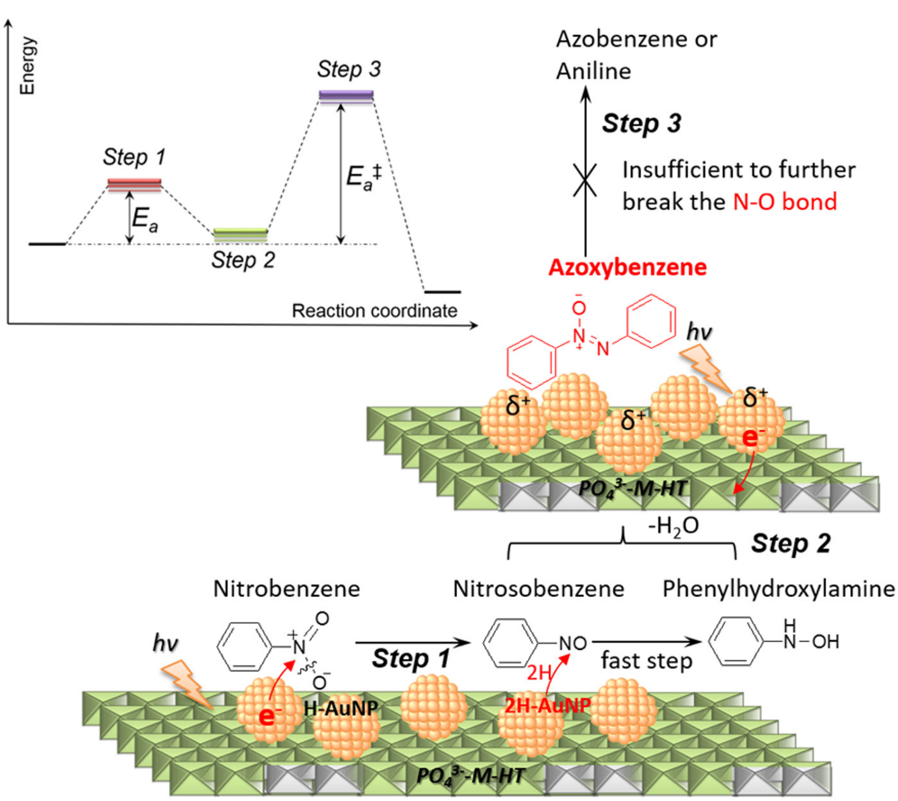

Scheme 2. Proposed mechanism for the photocatalytic reduction on Au/PO_4^{3-}-M-HT catalyst under irradiation. The inset on top left: schematically shows the reaction barriers (E_a and $E_a^‡$) to overcome for the specific steps to facilitate the reaction.

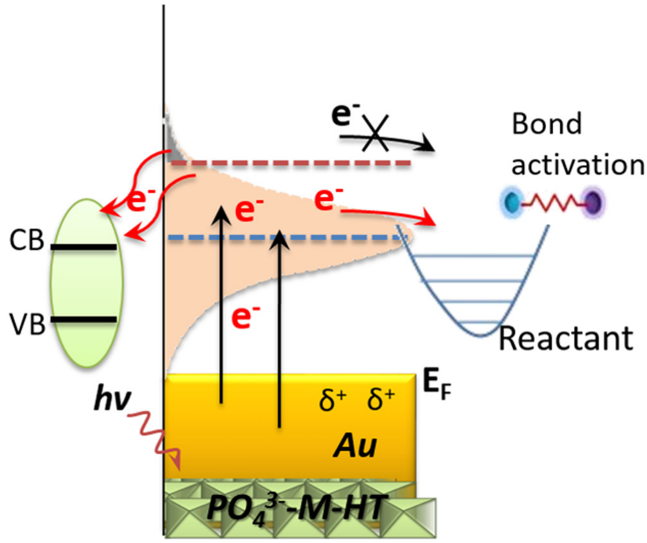

Scheme 3. Proposed light excited electron transfer mechanism for the photocatalytic process on Au NP catalyst with PO_4^{3-}-M-HT support under irradiation. The dashed blue line indicates the threshold of step 1 for the reduction of nitrobenzene to nitrosobenzene, and the dashed red line indicates the threshold of step 3 for the reduction of azoxybenzene to azobenzene. Only those electrons excited above the thresholds could be transferred into the reactant molecule to induce the reaction. (For interpretation of the references to colour in this figure legend, the reader is referred to the web version of this article.)

on the light intensity, observed in Fig. 7, usually suggests an electron-driven chemical process on metal NP surface [37]. Also, light-excited transient electrons can transfer from the NP surface to a chemically adsorbed molecule is well-known [44,45]. This means that the excited conduction electrons can interact strongly with the electrophilic nitro groups of nitrobenzene molecules, and assist the cleavage of the N—O bonds by the H-AuNP species on the AuNPs [46]. Increasing the irradiation intensity and temperature produces more excited electrons, which can results in higher conversion rates. Thus, nitrobenzene is firstly reduced to nitrosobenzene (Step 1), which then in turn is quickly converted to phenylhydroxylamine. Phenylhydroxylamine can readily couple with nitrosobenzne to form dihydroxy intermediate, which can dehydrate to give azoxybenzene (Step 2, Scheme 2). This is a very fast step (almost barrierless), the reaction could occur spontaneously and yield azoxybenzene [46].

The reaction did not proceed further to form azobenzene or aniline (Step 3), this is due to the reaction barrier of the hydrogenation of azoxybenzene to azobenzene is much higher than that of former steps (as schematically shown in the inset) [22,23]. Using detailed density functional theory (DFT) calculation, Gu et al. demonstrated that in the whole reduction process, only the initial step of nitrobenzene to nitrosobenzene and the step of azoxybenzene to azobenzene have relatively higher reaction barriers (0.27 eV and 0.56 eV, respectively) which are the reaction rate-limiting steps [23]. Thus, the former steps in the reduction can proceed smoothly with the light-excited electrons because of the lower reaction barriers (Step 1), whereas only those excited energetic electrons with higher energy can activate the N—O bond in azoxybenzene molecule to overcome the higher barrier to further achieve azobenzene or aniline (Step 3). We proposed the light excited electron transfer process for this steps (Scheme 3). Since there is an energetic requirement for light excited electron transfer: the electrons must have an energy above a threshold that depends on the energy level of the molecular orbital associated with the N—O bonds (two different thresholds for Step 1 and 3, respectively as shown in the dashed lines) [46,47]. The electrons with sufficient energy can be transferred into the reactant molecules for bond activation, resulting in the reaction.

We schematically proposed the light excited electron transfer mechanism for the photocatalytic process on Au NP catalyst with PO_4^{3-}-M-HT support under irradiation. As indicated in Scheme 3, the light excited electrons with sufficient energy could be transferred into the reactant for bond activation to initiate the reaction. Recently Carja and co-workers found that there are positive charges on the surface of the AuNPs on HT support [48]. They believed that those light-excited higher energy electrons may easily inject into the conduction band (CB) of HT (as indicated in Scheme 3), resulting in a population of Au surface with positive charge density. It is also report that the PO_4^{3-} species may increase the charge redistribution and internal electric field inside the support [29], which can facilitate the electron transfer. The positive surface charges on the AuNPs will strongly attract the hot electrons of AuNPs, and weaken their ability to interact with reactant molecules on the AuNP surface. Moreover, the resultant positive charged Au surface is unfavorable to interact with the electrophilic N—O bond. Both of these two aspects can explain the decreased reduction power for the reaction. Thus, overall the light excited electrons of AuNPs on the modified HT support can only provide sufficient energy above the threshold of Step 1 to activate the N—O bond for the reduction of nitrobenzene to nitrosobenzene, and few electrons could be populated above the threshold of Step 3 for further reaction. This is a preliminary result and needs to be explored further in future work.

4. Conclusions

In conclusion, an environmental sustainable and industrial friendly visible light driven process for azoxy-compounds production has been developed using modified hydrotalcite-supported gold nanoparticles. We can reduce the reduction power of the photocatalyst by introducing phosphate and metal ions into the support, to prevent the reduction of azoxy-compounds to azo-compounds and anilines and achieve excellent selectivity to azoxy-compounds. The moderate reaction conditions and the synergistic effect of the modified HT support ensure the efficient and green process yielding azoxy-compounds. The results show that controlled manipulation of the reaction selectivity via the tailoring catalyst support is a new and effective strategy towards the development of versatile heterogeneous photocatalysts.

Acknowledgements

We thank Australian Research Council for the financial support (ARC DP110104990 and DP150102110); Arixin Bo for performing the SEM and EDX analysis; and Dr Barry Wood from UQ for performing the XPS analysis.

Appendix A. Supplementary data

Supplementary data associated with this article can be found, in the online version, at http://dx.doi.org/10.1016/j.apcatb.2017.03.002.

References

[1] E.R. Burkhardt, K. Matos, Chem. Rev. 106 (2006) 2617.
[2] A.M. Tafesh, J. Weiguny, Chem. Rev. 96 (1996) 2035.
[3] G.S. Kumar, D.C. Neckers, Chem. Rev. 89 (1989) 1915.
[4] S. Ghosh, S.S. Acharyya, T. Sasaki, R. Bal, Green Chem. 17 (2015) 1867.
[5] E. Buncel, Can. J. Chem. 78 (2000) 1251.
[6] E. Buncel, Acc. Chem. Res. 6 (1975) 132.
[7] F.A. Khan, Ch. Sudheer, Tetrahedron Lett. 50 (2009) 3394.
[8] J.R. Hwu, A.R. Das, C.W. Yang, J.-J. Huang, M.-H. Hsu, Org. Lett. 7 (2005) 3211.
[9] Ch. Srilakshmi, H.V. Kumar, K. Praveena, C. Shivakumara, M.M. Nayak, RSC Adv. 4 (2014) 18881.

[10] Y. Liu, B. Liu, A. Guo, Z. Dong, S. Jin, Y. Lu, Synth. Commun. 42 (2012) 2201.
[11] H.Q. Li, X. Liu, Q. Zhang, S.-S. Li, Y.-M. Liu, H.-Y. He, Y. Cao, Chem. Commun. 51 (2015) 11217.
[12] X. Liu, H.Q. Li, S. Ye, Y.M. Liu, H.Y. He, Y. Cao, Angew. Chem. Int. Ed. 53 (2014) 7624.
[13] A. Grirrane, A. Corma, H. Garcia, Science 322 (2008) 1661.
[14] R.V. Jagadeesh, A.E. Surkus, H. Junge, M.M. Pohl, J. Radnik, J. Rabeah, H.M. Huan, V. Schunemann, A. Bruckner, M. Beller, Science 342 (2013) 1073.
[15] A. Albini, E. Fasani, M. Moroni, S. Pietra, J. Org. Chem. 51 (1986) 88.
[16] M. Cifelli, G. Cinacchi, L. De Gaetani, J. Chem. Phys. 125 (2006) 164912.
[17] H.Y. Zhu, X.B. Ke, X.Z. Yang, S. Sarina, H.W. Liu, Angew. Chem. Int. Ed. 49 (2010) 9657.
[18] X.B. Ke, X.G. Zhang, J. Zhao, S. Sarina, J. Barry, H.Y. Zhu, Green Chem. 15 (2013) 236.
[19] Q. Xiao, E. Jaatinen, H. Zhu, Chem. Asian J. 9 (2014) 3046.
[20] S. Sarina, E.R. Waclawik, H. Zhu, Green. Chem. 15 (2013) 1814.
[21] X. Guo, C. Hao, G. Jin, H.-Y. Zhu, X.-Y. Guo, Angew. Chem. Int. Ed. 53 (2014) 1973.
[22] A. Corma, P. Concepción, P. Serna, Angew. Chem. Int. Ed. 46 (2007) 7266.
[23] L. Hu, X. Cao, L. Chen, J. Zheng, J. Lu, X. Sun, H. Gu, Chem. Commun. 48 (2012) 3445.
[24] N.K. Gupta, S. Nishimura, A. Takagaki, K. Ebitani, Green Chem. 13 (2011) 824.
[25] A. Noujima, T. Mitsudome, T. Mizugaki, K. Jitsukawa, K. Kaneda, Angew. Chem. Int. Ed. 50 (2011) 2986.
[26] D.P. Debecker, E.M. Gaigneaux, G. Busca, Chem. Eur. J. 15 (2009) 3920.
[27] Q. Xiao, Z. Liu, A. Bo, S. Zavahir, S. Sarina, S. Bottle, J.D. Riches, H. Zhu, J. Am. Chem. Soc. 137 (2015) 1956.
[28] P. Liu, Y. Guan, R. van Santen, C. Li, E.J.M. Hensen, Chem. Commun. 47 (2011) 11540.
[29] W.J. Jo, J.W. Jang, K.J. Kong, H.J. Kang, J.Y. Kim, H. Jun, K.P.S. Parmar, J.S. Lee, Angew. Chem. Int. Ed. 51 (2012) 3147.
[30] M.C.I. Bezen, C. Breitkopf, J.A. Lercher, ACS Catal. 1 (2011) 1384.
[31] J. Orthman, H.Y. Zhu, G.Q. Lu, Sep. Purif. Technol. 31 (2003) 53.
[32] S. Sarina, H. Zhu, E. Jaatinen, Q. Xiao, H. Liu, J. Jia, C. Chen, J. Zhao, J. Am. Chem. Soc. 135 (2013) 5793.
[33] Q. Xiao, S. Sarina, E. Jaatinen, J. Jia, D.P. Arnold, H. Liu, H. Zhu, Green. Chem. 16 (2014) 4272.
[34] Q. Xiao, S. Sarina, A. Bo, J. Jia, H. Liu, D.P. Arnold, Y. Huang, H. Wu, H.Y. Zhu, ACS Catal. 4 (2014) 1725.
[35] F.Z. Su, L. He, J. Ni, Y. Cao, H.Y. He, K.N. Fan, Chem. Commun. 30 (2008) 3531–3533.
[36] J. Liu, Y. Yang, N. Liu, Y. Liu, H. Huang, Z. Kang, Green Chem. 16 (2014) 4559.
[37] I. Cano, M.A. Huertos, A.M. Chapman, G. Buntkowsky, T. Gutmann, P.B. Groszewicz, P.W.N.M. van Leeuwen, J. Am. Chem. Soc. 137 (2015) 7718.
[38] P. Christopher, H.L. Xin, A. Marimuthu, S. Linic, Nat. Mater. 11 (2012) 1044.
[39] S. Linic, P. Christopher, D.B. Ingram, Nat. Mater. 10 (2011) 911.
[40] M.J. Kale, T. Avanesian, P. Christopher, ACS Catal. 4 (2014) 116.
[41] F.Z. Haber, Elektrochem. Angew. Phys. Chem. 4 (1898) 506.
[42] H.U. Blaser, Science 313 (2006) 312.
[43] D.K. Roper, W. Ahn, M. Hoepfner, J. Phys. Chem. C 111 (2007) 3636.
[44] L. Brus, Acc. Chem. Res. 41 (2008) 1742.
[45] C.D. Lindstrom, X.Y. Zhu, Chem. Rev. 106 (2006) 4281.
[46] Q. Xiao, S. Sarina, E.R. Waclawik, J. Jia, J. Chang, J.D. Riches, H. Wu, Z. Zheng, H. Zhu, ACS Catal. 6 (2016) 1744.
[47] J.G. Smith, J.A. Faucheaux, P.K. Jain, Nano Today 10 (2015) 67.
[48] G. Carja, M. Birsanu, K. Okadac, H. Garcia, J. Mater. Chem. A 1 (2013) 9092.